Deciphering the Adsorption Mechanisms of RGD Subunits: L-Aspartic Acid on Cu(110)

Roberta Totani, Christophe Méthivier, Hervé Cruguel, Claire-Marie Pradier, Vincent Humblot

Deciphering the Adsorption Mechanisms of RGD Subunits: L-Aspartic Acid on Cu(110)

*Roberta Totani[1], Christophe Méthivier[1], Hervé Cruguel[2], Claire-Marie Pradier[1] and Vincent Humblot[1]**

[1] Sorbonne Universités, UPMC Université Pierre et Marie Curie, Univ Paris 6, Paris, France, Laboratoire de Réactivité de Surface LRS - UMR CNRS 7197, 4 place Jussieu, F-75005 Paris, France

[2] Sorbonne Universités, UPMC Université Pierre et Marie Curie, Univ Paris 6, Paris, France, Institut des NanoScience de Paris INSP - UMR CNRS 7588, 4 place Jussieu, F-75005 Paris, France.

ABSTRACT

In this work we present a detailed surface science characterization of L-Aspartic acid adsorption on a Cu(110) surface. Aspartic acid is one of the main components of the tri-peptide RGD (arginine-glycine-aspartic acid). We replaced the traditional sublimation method to obtain molecular films by dosing aspartic acid directly from an aqueous solution through an Electrospray Ionization (ESI) device. X-ray Photoelectron Spectroscopy (XPS) and Polarization Modulation Reflection Absorption Infra Red Spectroscopy (PM-RAIRS) evidenced different

adsorption states ranging from sub-monolayer regime up to multilayers. Molecules-substrate interactions guide the creation of the pattern observed in the sub-monolayer, but molecule-molecule interactions are prevailing from a certain coverage stage, promoting the overlayer growth while leaving exposed areas of bare copper. This is evidenced by Scanning Tunneling Microscopy (STM) results, showing that single aspartic acid molecules self-organize in a 2D chiral network at low coverage and start originating new molecular layers even before a saturated monolayer has been reached.

INTRODUCTION

A better knowledge and control of biomolecule-metal interactions is a central issue for the rational design of biocompatible and/or protein-resistant materials. Fundamental research is always at the intermediate position between a fully understanding of small molecule adsorption on well-defined surfaces ("ideal" surface science approach) and "post mortem" characterization of real biological systems ("real" approach). In this context, we put our effort on the study of the adsorption of small biomolecules, namely amino acids and small di- or tri-peptides, on metallic single crystal surfaces, most often by applying a surface science approach.

We have recently shown that molecules dosed via an electrospray ionization (ESI) device are adsorbed intact and in a chemical state close to that in solution.[1,2] Compared to the traditional Knudsen cells, ESI allows an adsorption from an aqueous solution at room temperature; high sublimation temperatures are thus avoided and molecular films of delicate biomolecules can be obtained without any molecular damage. Our next objective is to unravel the interaction modalities of more relevant peptides, like RGD, which plays a determining role in the context of biotechnologies for its capacity to promote cell adhesion or other peptide sequences for specific

molecular recognition or cell interactions on metallic or oxidized surfaces[3]. RGD is currently employed for biomaterials functionalization and knowledge of RGD adsorption mechanisms on different surfaces is of paramount importance for its implementation. The tri-peptide RGD is constituted of three amino acids, namely arginine, glycine and aspartic acid (ASP). Arginine and ASP, differently from glycine,[4,5,6,7,8,9] have not given rise to extended investigations of their interaction with a metal surface.

As a first step in the characterization of RGD interaction with a copper surface, we studied ASP adsorption on a Cu(110) surface. Moreover, considering that RGD, a rather heavy tri-peptide, will not be easily sublimated in the UHV chamber, an ESI device will probably be necessary to introduce RGD with no damage. Therefore, we have already used the ESI device for ASP in order to keep similar evaporation conditions.

ASP, $C_4H_7NO_4$ (Figure 1), is mostly known for being one of the main ingredients of the artificial sweetener *aspartame*, together with L-phenylalanine. What is maybe less known is that is one of the most abundant amino acids in nature, it has fundamental biological and biomedical/biotechnological functions[10, 11, 12, 13, 14, 15] and, last but not the least, is the C-ter end of RGD.

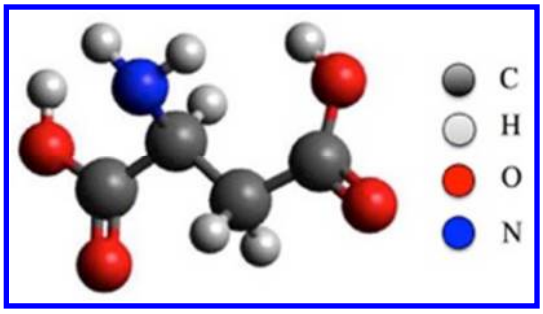

Figure 1. Schematic representation of an L-aspartic acid molecule.

From a chemical point of view, ASP contains an amine group and two distinct carboxylic acids at its two extremities. It has been extensively studied, theoretically and experimentally, on

oxyhydroxide surfaces, like TiO_2[16, 17] and Al_2O_3,[18] in view of possible applications in various fields of interest, ranging from biomedical devices to earth science and astrobiology. Most of these studies were performed *ex-situ*, by coating aspartic acid in solutions on the substrates, followed by sample characterization.

Studies of ASP on metallic substrates and in ultra-high vacuum (UHV) conditions are quite rare. ASP has been adsorbed on Ni(111) surfaces, from solution[19] and by sublimation,[20] as a surface chiral modifier to investigate the enantioselective hydrogenation of β – ketoesters. More recently, Gellman and co-workers have studied ASP films evaporated (in racemic mixture or as pure D or L enantiomers) in UHV conditions, to characterize the enantiomer nature of ASP molecules on chiral and achiral copper surfaces.[21, 22, 23, 24, 25] All these studies have in common the conclusion that ASP chemical form after adsorption on a surface depends on the film coverage. However, this form is different according to the substrate. On Ni surfaces, ASP is in its zwitterionic (COO^-/NH_3^+) form at lower coverages, and in its anionic (COO^-/NH_2) form at high coverages.[20] On Cu surfaces, ASP is found with two COO^- groups and a neutral (NH_2) amine group for lower coverage and in its zwitterionic form for higher coverage.[25] The doubly-deprotonated carboxylic groups and the neutral amine group of the lower coverage are considered the responsible for the ASP anchorage on the surface.

This work aims at studying the adsorption mechanisms of L-ASP after deposition by ESI on Cu(110) surfaces. The chemical state and the anchoring points of the molecules on the surface, deduced through X-ray Photoelectron Spectroscopy (XPS) and Polarization Modulation Infrared Reflection Absorption Spectroscopy (PM-RAIRS) revealed, also in this case, changes in the chemical state, charge and configuration of ASP molecules, with the coverage. Scanning Tunneling Microscopy (STM) furnished complementary information about the layer structure,

showing the creations of a chiral 2D network for submonolayer coverage, determined by molecule-substrate interactions, and the growth of the overlayer before reaching a saturated monolayer, with a prevalence of molecule-molecule interactions.

EXPERIMENTAL SECTION

All measurements were performed in UHV conditions, *i.e.* with a base pressure better than $1x10^{-10}$ mbar, with the sample kept at room temperature. PM-RAIRS and XPS measurements were realized *in situ*. STM images were acquired after dosing using a different experimental equipment.

Materials. Before ASP adsorption, the Cu(110) crystal (Surface Preparation Laboratory, The Netherlands, purity of 99.99% (4N) and alignment accuracies of 0.1°) was prepared for the experiments through several cycles of Ar^+ sputtering (500 eV, $P_{Ar}=3x10^{-6}$ mbar) and annealing at 850 K. XPS and LEED (Low Energy Electron Diffraction) were used to check surface cleanliness and reconstruction. L-ASP was purchased by Fluka (99%) and used without further purification.

Dosing. ASP adsorption has been realized from a 1 mM solution of ASP in a methanol/water 75:25 ratio by means of an ESI device. Explanations on ESI mode and principles of operation can be found elsewhere.[1,2]**Error! Bookmark not defined.** Dosing of 2, 5 and 7 minutes for XPS and 2 and 5 minutes for STM were used to obtain different ASP coverage. The pressure during the dosing varied in the range $1x10^{-7}$ to $5x10^{-7}$, with a base pressure of $7x10^{-8}$ after opening the gate valve between the ESI vessel and the experimental chamber. A positive voltage of 1.5 kV was applied, with ASP gas phase molecules nominally in their cationic state, *i.e.* $COOH/NH_3^+$.

Thickness evaluation. The thickness *d* of the obtained molecular layer could be estimated by means of the intensities ratio IC1s/ICu2p of C1s and Cu2p XPS spectra, related by the formula:

$$\frac{IC1s}{ICu2p} = \frac{T_{C1s}}{T_{Cu2p}} \frac{\sigma_{C1s}}{\sigma_{Cu2p}} \frac{\lambda_{C1s}^{ad} C_{C1s}^{ad} \left[1 - exp\left(\frac{-d}{\lambda_{C1s}^{ad} cos\theta}\right)\right]}{\lambda_{Cu2p}^{su} C_{Cu2p}^{su} exp\left(\frac{-d}{\lambda_{Cu2p}^{ad} cos\theta}\right)} \quad [1]$$

where $cos\theta$ is 1 because the photoelectron collection angle θ is equal to zero. T_{C1s} and T_{Cu2p} are the relative sensitivity factors of C and Cu, respectively, provided by the spectrometer manufacturer. The Scofield photoionization cross sections σ are 1 for C 1s and 2.48 for Cu 2p. The superscripts *ad* and *su* designate the adsorbed layer and the copper substrate, respectively. C_x^y represents the concentration of the element x in the matrix y. The electron inelastic mean free paths λ were calculated using the Quases program based on the TPP2M formula.[26] For more details on equation [1], see Supp. Info section.

PM-RAIRS. Spectra were recorded using a Nicolet 5700 spectrometer equipped with a nitrogen-cooled MCT wide-band detector. A ZnSe grid polarizer and ZnSe photoelastic modulator to modulate the incident beam between p and s polarization were placed prior to the sample. The spectrometer was interfaced to the UHV chamber via ZnSe windows. The reflected light was focused onto the detector at an optimal incident angle of 85°. All spectra were obtained after 1024 scans with a resolution of 8 cm^{-1}.

XPS. Photoemission analysis was performed using a SPECS (Phoibos 100 1D Delay Line Detector) hemispherical analyzer and a monochromatized aluminum K_α X-ray source (hν = 1486.6 eV). The acquired spectra were calibrated according to the Cu Fermi level. The experimental uncertainty on the position in biding energy of the XPS peaks is 0.1 eV.

STM. STM experiments were conducted in an Omicron Vakuumphysik XA VT-STM chamber with facilities for STM, LEED and sample cleaning. All STM images were acquired in constant current mode. The STM scanner was calibrated using the Cu(110)-O-(2×1) missing/added rows (interspacing distance = 0.51 nm).

RESULTS AND DISCUSSION

PM-RAIRS spectra obtained after a 2, 5 and 7 minutes dosing by ESI are shown in Figure 2a, together with the peak assignment (Figure 2b) in agreement with previous ASP infrared studies[27] and with the infrared analysis of ASP solutions at different pHs (see the Supporting Information section, Figure S1). One can notice three main features at 1427 cm^{-1}, 1391 cm^{-1} and 1352 cm^{-1}, present on the PM-RAIRS spectra at all examined coverages. The sharp bands at 1427 cm^{-1} and 1391 cm^{-1} are attributed to the symmetric stretching vibrations of, respectively, the α-carboxylate (closer to the amine group) and the distal carboxylate functionalities (Figure S1). The not symmetric position of the amine group in the molecule breaks the degeneracy of the two otherwise equivalent COO^- groups and leads to two distinguishable contributions. The observed vibrations also furnish a direct evidence of the carboxylic acids deprotonation. As already reported for other copper surfaces,[28] the hydrogen atoms released by protonation processes undergo recombinative desorption as hydrogen molecules

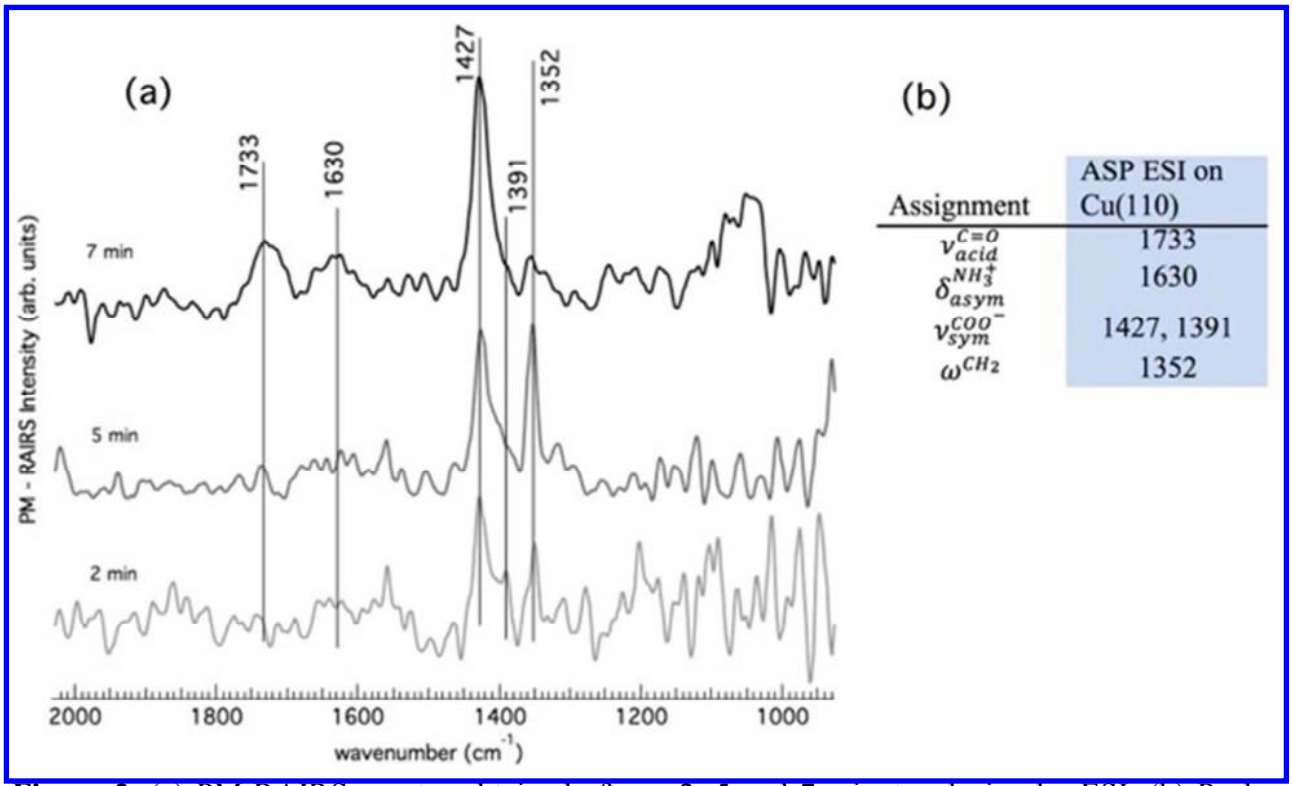

Figure 2. (a) PM-RAIRS spectra obtained after a 2, 5 and 7 minutes dosing by ESI; (b) Peak assignment table.

The third rather intense band at 1352 cm^{-1} can be ascribed to the CH_2 wagging mode.[20] Increasing the molecular coverage on the substrate, one observes two other bands growing. The C=O stretching mode and the NH_3^+ asymmetric deformations, visible in the 7 minutes adsorption spectrum in Figure 2a, are responsible for the broad features at 1733 cm^{-1} and 1630 cm^{-1}, respectively. Additional information concerning the (protonated or not) nature of the amino group will be given by analyzing the XPS data.

The N1s and O1s XPS spectra obtained at the three investigated dosing times are shown in Figure 3. The spectra and the subsequent analysis are in perfect agreement with a previous study of ASP sublimated on Cu(110),[25] confirming once again that ESI is as accurate and reproducible, in term of sample preparation methods, as traditional sublimation. For nitrogen, Figure 3b, in the 2 minutes adsorption spectrum, the Binding Energy (BE) of the N1s peak at 399.9 eV is

characteristic of the neutral amino NH_2 group; a peak at higher binding energy, 402.1 eV, is visible and intense after longer times of exposure (5 and 7 minutes), attributed to the protonated NH_3^+ groups.[25,29 30, 31,32]

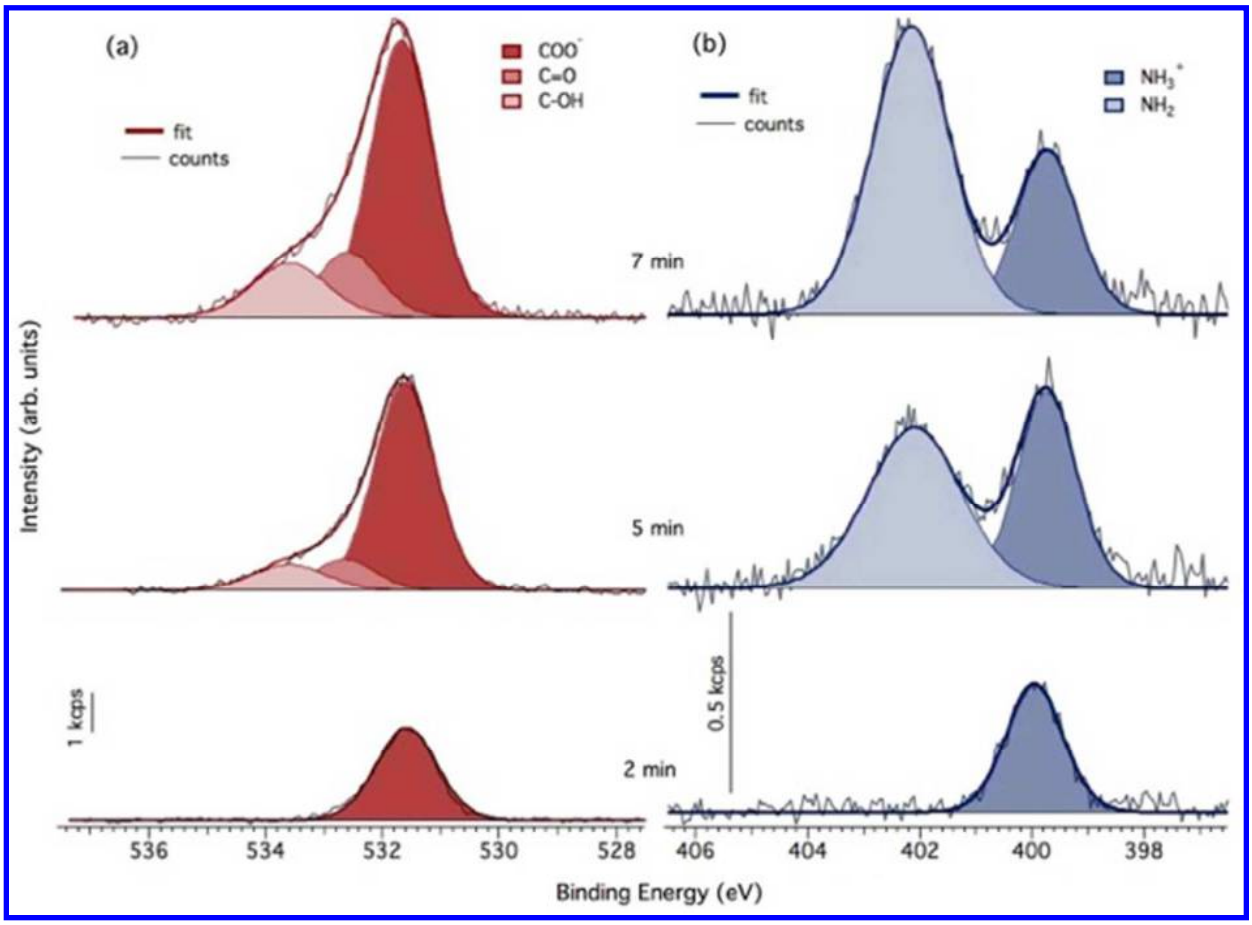

Figure 3. Evolution of ASP O1s (a) and N1s (b) XPS peaks, for increasing molecular coverage. The fitting procedure to disentangle the contributions of the different species to the core level spectra is also shown.

At the same time, the presence of the NH_2 peak, alone, suggests that the initial interaction of the molecule with the surface induces a deprotonation of all NH_3^+ groups existing in the gas phase. Consistently, for oxygen (Figure 3a), a unique O1s peak at 531.7 eV, ascribed to the COO^- group oxygen, indicates a deprotonation of COOH groups, confirming the interaction of the

carboxylate groups with the surface, as deduced from infrared data (Figure 2). One has to point out that the cationic state of ASP molecules obtained through ESI is an assumption based on the ESI working principles. In fact, in lacking of gas phase measurements on the ESI beam, we cannot exclude the possibility that molecules are in a different state. In particular, the obtained data would be also consistent with neutral ($COOH/NH_2$) ASP molecules arriving on the surface. For the 2 minutes results, this would simply imply that no deprotonation occurs in the amine group, while keeping the same interaction mechanisms for the carboxylic groups. After 5 minute dosing, the N 1s spectrum displays two peaks, indicating that the NH_3^+ groups now exist in the adsorbed molecules. Together with this change in the N1s peak, two peaks on the high binding energy tail of the COO^- peak start to be visible on the O1s spectrum, at 532.9 and 533.6 eV respectively. These are the contributions from C=O and C-OH oxygen atoms,[33,34] suggesting the presence of COOH. Note that these two contributions have equal intensities, and their relative intensities increase from 5 to 7 minutes (12 % to 16 % of the total O1s intensity). The C 1s spectra for the three dosing times, shown in the Supporting Information section (Figure S2), are in agreement with O1s data, confirming COOH complete deprotonation for low coverage and COOH neutral state, coexisting with some COO^-, for higher coverages. Eventually, the values of the average coverage values, calculated from the attenuation of the copper signal (Equation 1), lead to the following numbers: 3.2 Å, 6.7 Å and 10 Å after 2, 5 and 7 minutes of dosing, respectively. Estimating a maximum size for ASP molecules of 5 Å (maximum gas phase elongation), one may think that after 2 minutes of exposures, only a fraction of monolayer is on the surface whilst multilayer starts to grow after 5 minutes of exposure. This will be later confirmed by STM images.

The appearance of the NH_3^+, C-OH and C=O peaks after 5 minute dosing is in agreement with the building of multilayers where molecules do not interact directly with the surface, thus do not undergo a deprotonation of COOH and NH_3^+ groups. Alternatively, in the presence of neutral gas phase molecules, the 5 and 7 minutes results would infer the creation of a zwitterionic network in the multilayer, with one deprotonated carboxylic group in interaction with the positively charged amine group and the second carboxylic group still in its neutral state. Another possibility would be the NH_2 group of the monolayer turning into NH_3^+ and interacting with a COO^- group of the second layer. Both situations are consistent with the high binding energy contributions observed in O, N and C 1s spectra for higher coverages. The process determining the state of the amine (carboxylic) group would not be an actual protonation (deprotonation) but a delocalization of the proton, favored by the amine (acid) nature of the functional group.

Gathering all the information obtained so far and considering the strict RAIRS dipole selection rules, which allow observing only vibrational modes with a dynamic dipole moment non-parallel to the surface,[35] we can deduce some characteristics of the geometries of adsorbed ASP molecules depending on the coverage. In the submonolayer regime (2 minutes dosing), the intense symmetric COO^- band and the almost absence of absorption at ca 1600 cm^{-1} suggest that the four oxygen atoms from the COO^- groups are anchored to the surface in a bidentate configuration. A similar geometry was observed for bitartrate[36] and bisuccinate[37] on Cu(110) and it is also in agreement with the geometry proposed in previous ASP studies.[24,25] Besides that, looking at the different intensities of the carboxylate bands at 1391 and 1427 cm^{-1} (Figure 2a), we can say that the OCO planes positions, even if close to be normal to the surface plane, are slightly different, with the distal carboxylate plane less perpendicular than the α-carboxylate plane with respect to the surface and thus less contributing to the infrared spectral intensity.

Differently from studies from Gellman's group,[24,25] we hypothesize that the NH_2 amine group is not interacting with the surface. In fact, since no contribution from the NH_2 group is visible in corresponding infrared data, we deduce that, at low coverage, its plane is parallel, or almost parallel, to the surface. Besides, N1s 2 minutes spectrum (Figure 3a) denotes the absence of interactions between NH_2 and Cu, otherwise a peak at lower binding energies would have been visible, due to hydrogen bonds, -N-H—Cu, between the amine group and the Cu surface, as already been observed in similar studied on copper1 and on gold surfaces.[30,38] After 5 minutes adsorption the α-carboxylate band increases, while the distal carboxylate band remains constant (Figure 2a), thus suggesting a slight reorientation of the former carboxylate in a more perpendicular position and of the latter carboxylate in a more parallel position with respect to the substrate. Finally, the appearance of the C=O stretching mode and of the NH_3^+ asymmetric deformations bands and the decreasing of the CH_2 wagging band intensity in the 7 minutes adsorption infrared spectrum suggests that, once the multilayer regime is reached, molecules are found in various orientations, some letting COOH and NH_3^+ planes more perpendicular and CH_2 planes more parallel to the surface. Changes in molecular arrangement when the coverage increases is a commonly observed phenomenon, already encountered, for alanine,[39] tartaric acid,[36] lysine[40] and methionine[31] on Cu(110).

Figure 4 presents the STM images corresponding to a submonolayer of ASP on the Cu(110) surface; one can see on Figure 4a that ASP tends to originate organized structures forming islands on the surface. A closer look into one of the islands (Figure 4b) reveals that those are made of "bilobate" elements. Tracing several line profiles longitudinally along the elements (line profile 1, Figure 4c, we discovered that the two lobes are (3.7 ± 0.4) Å apart and one is at a slightly different z position with respect to the other.

As pointed out from infrared results, OCO planes of the two ASP carboxylate groups are characterized by a different angle with respect the substrate, being the α-carboxylate -$^{-}$OOC-NH_2 group more perpendicular than the distal –COO^- group to the surface. In this way, the two extremities of the molecule are forced to be at a different distance (*i.e.* height) from the surface. Therefore, we propose that the two lobes at different z position revealed by STM profiles correspond to the two ends of a single ASP molecule, with the highest lobe being the end with the distal α-carboxylate -$^{-}$OOC-NH_2. An analogous situation has been observed for methionine on Au(111)[41] where a single methionine molecule appeared as two bright spots, due to the fact that, as evidenced by DFT calculations, the sulfur moiety and the carboxylic acid groups had different orientations, pointing towards and away from the surface, respectively. Besides, the distance between the two lobes in ASP is comparable to the distance between the two bright dots in methionine, while is half the distance observed, for example, between the two bright spots characterizing lysine pattern on Cu(110).[40] However, differently from methionine, lysine tends to self-organize in dimers. So the bigger distance between its two double features confirms the hypothesis of ASP single-molecule assembly.

A further statistical analysis revealed the distances between ASP molecules along the main symmetry directions of the 2D pattern (line profiles 2 and 3 of Figure 4b, shown in Figure 4c), which are, on average, (10.7±0.5) Å and (13.0±0.5) Å.

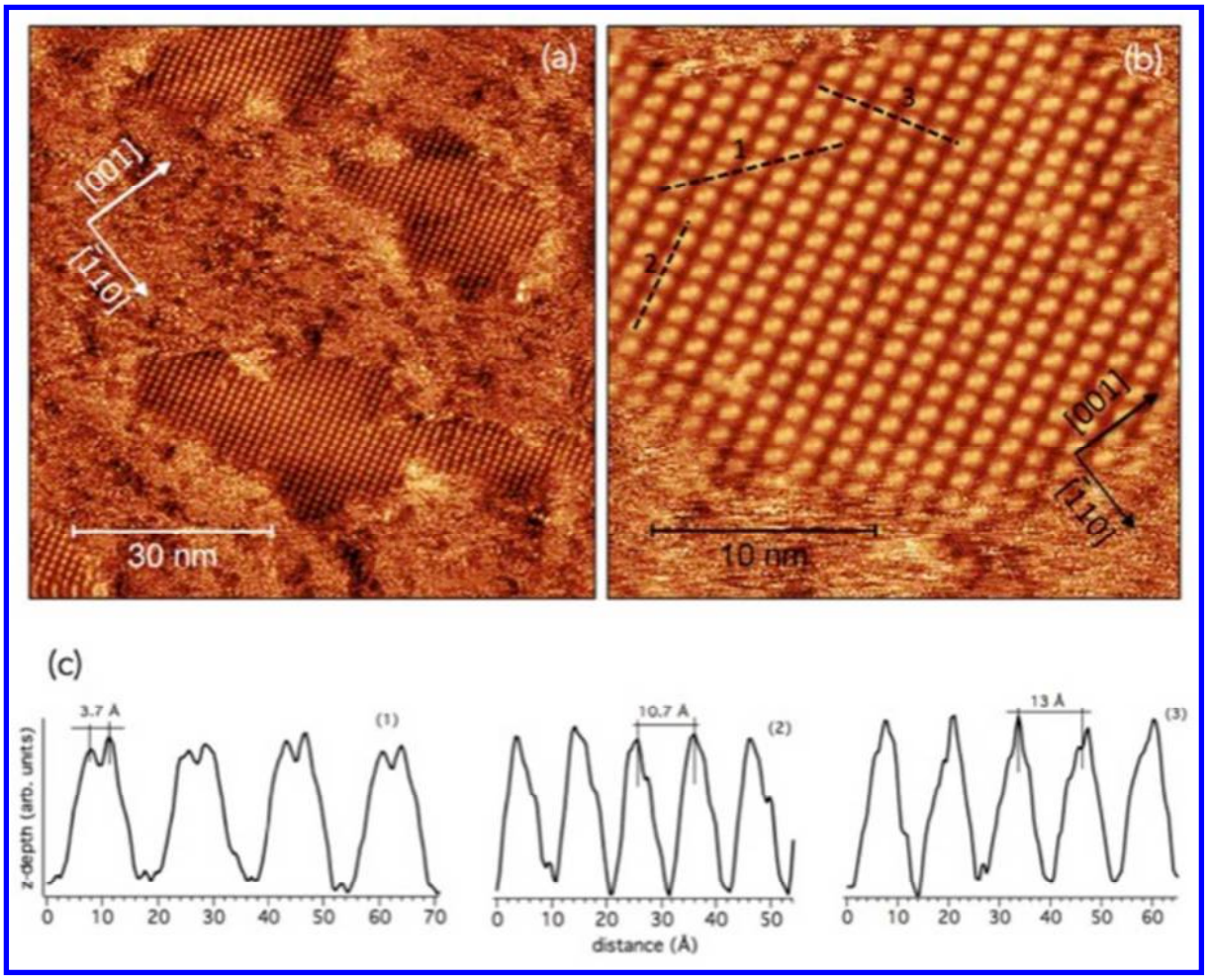

Figure 4. (a) Islands of ASP molecules, characteristics of the submonolayer regime. (b) Bilobate elements inside ASP islands. (c) Profiles extracted from dashed lines in (b). Image conditions are: (a) 84 nm x 85 nm, V = 1.1 V, I = 100 pA, (b) 25.2 nm x 25.5 nm, V = 1.1 V, 120 pA.

Comparing these experimental measurements and the distance between the two lobes with the crystallographic data, respectively, 1.11 nm, 1.33 nm and 0.44 nm, we are able to show a schematic representation of ASP molecules adsorbed on the Cu(110) rows and of the unit cell (Figure 5a), with the unit vectors represented by the (-1, 3; -5, 1) matrix. ASP molecules are adsorbed diagonally across the closed-packed rows (Figure 5b) in the bidentate configuration already discussed in the XPS/PM-RAIRS section.

The distance between 2 neighboring ASP molecules, bigger than the weakest hydrogen bond (roughly 4 Å[42]), and their anionic (COO^-/NH_2) state on the surface, prevent the creation of any intermolecular hydrogen-bonding network. A similar situation with methionine adsorbed on Cu(110) led to a total absence of the 2D array.[31] Therefore, given the lacking of intermolecular directions, we propose that molecule-substrate interactions, rather than molecule-molecule interactions, are the driving force of the supramolecular assembly. The strict geometry adsorption via the four O atoms, indicating a not-negligible ASP-Cu interaction, seems to corroborate this suggestion.

It has to be noted that ASP molecules are accommodated along nonsymmetry directions, destroying the symmetry planes of the underlying substrate. In this way the surface is bestowed not only of point chirality due to the intrinsic chirality of ASP molecules, but also of chirality at the organizational level. Besides, since domains of different chirality are not present on the surface, we can conclude that the supramolecular assembly originated by ASP is able to modify an achiral surface such as Cu(110) into a truly chiral surface with a global chirality, as also observed, for example, in the adsorption of Gly-Pro on Cu(110).[36,39,43]

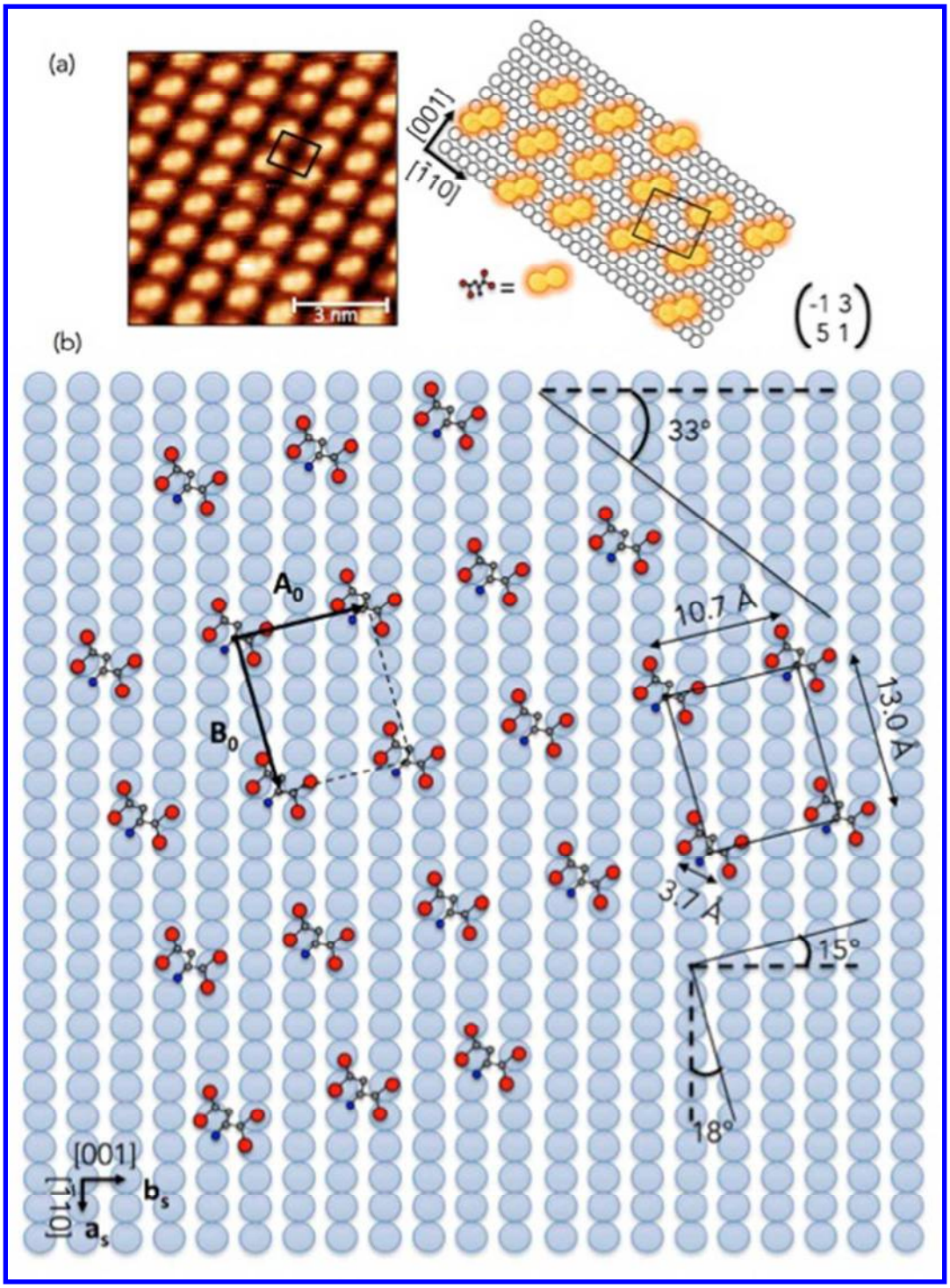

Figure 5. (a) ASP molecules 2D pattern from a high-resolution STM image (left, image conditions: 8.4 nm x 8.5 nm, 1.1 V, 120 pA) and depicted on copper rows in a schematic representation, together with the unit cell (right). (b) Adsorption model of ASP molecules, showing unit cell dimensions and the angles between the main symmetry directions of ASP pattern and Cu(110) crystallographic axis.

When the coverage increases (5 minutes dosing), ASP 2D pattern gradually covers the whole surface (Figure 6a). In the high resolution image shown in Figure 6b, we can identify the lighter areas as the beginning of the multilayer and fuzzy and not well-resolved areas (indicated by dashed arrows), ascribable to Cu(110) surface. We do not have enough elements to examine properly the multilayer pattern which, nonetheless, seems to be the characterized by more than one structure, as indicated by solid arrows in Figure 6b. However, we can clearly see that, even if the substrate is not still completely covered by the adsorbates, ASP molecules prefer accommodating on other molecules rather than on the bare surface. Line profile of Figure6c traced along the solid line of Figure 6b shows the simultaneous presence of the substrate, the monolayer and the starting overlayer. The multilayer way of growth can be explained considering that, since molecules in the overlayer are not interacting with the surface, there is no deprotonation of COOH/NH_3^+ groups in the case of cationic gas phase molecules or of COOH groups in the case of neutral gas phase molecules. Thus, differently from what seen in submonolayer regime, they have the possibility of hydrogen bonding creation that can favor the overlayer growth over the reaching of a saturated monolayer. Thus, this second stage of growth is characterized by a prevalence of ASP-ASP interactions over ASP-Cu interactions.

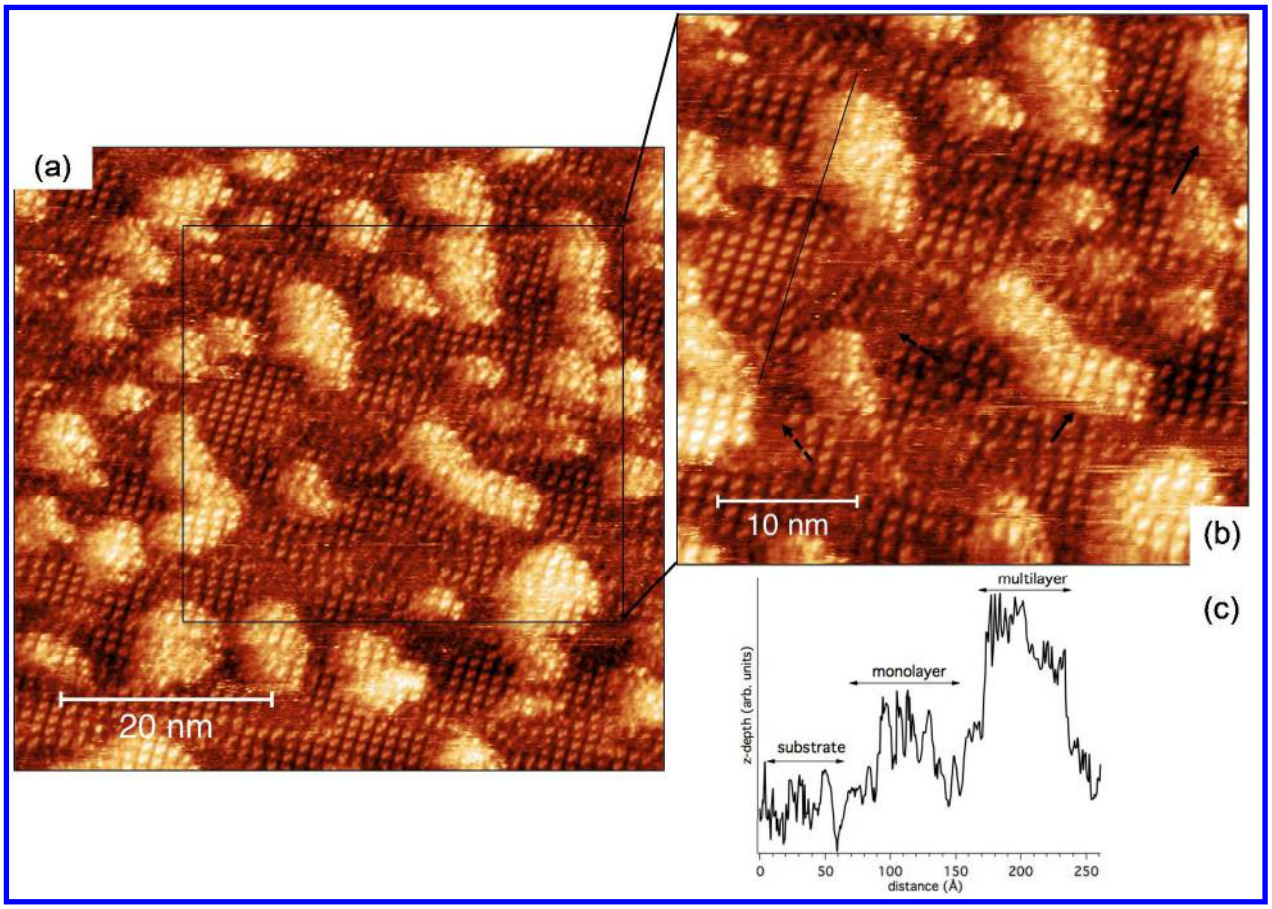

Figure 6. (a) Higher coverage (5 minutes dosing) of ASP: the ASP islands increase in number until reaching an almost complete covering of the underlying substrate. (b) High resolution STM image showing the co-existence of the multilayer (brighter areas) and of the Cu substrate, indicated by dashed arrows. Solid arrows indicate different co-existing multilayer structures. (c) Profile along the solid line traced in (b) to evidence the three elements present on the surface, substrate, monolayer and multilayer, and their different z position. Image conditions are: (a) 60.8 nm x 58.5 nm, 1.1 V, 50 pA; (b) 40.5 nm x 39 nm, 1.1 V, 50 pA.

CONCLUSIONS

We have realized the first surface science characterization of ASP films obtained by means of an ESI source. When aspartic acid is adsorbed on a Cu(110) surface, applying to the ESI a positive voltage, changes its state from cationic ($COOH/NH_3^+$) or neutral ($COOH/NH_2$) in the gas phase to anionic (NH_2/COO^-) on the surface. This implies that, respectively, either both the carboxylic acid groups and the protonated amine group or only the carboxylic acid group

undergo to a deprotonation process. As evidenced by our XPS and PM-RAIRS characterizations, when the molecular coverage increases, molecules are adsorbed in their gas phase state. This infers that the interaction with Cu is responsible for the hydrogen loss in the molecule. Besides, the higher presence of hydrogen facilitates the growth of the multilayer, with the formation of a NH_3^+--COO- hydrogen bonding network.

STM images, taken in the submonolayer regime (2 minutes dosing), show the creation of ASP islands inside Cu terraces. Each island is made of ASP molecules arranged along a nonsymmetry direction, diagonally crossing the close-packed rows and creating a chiral 2D network. In the 5 minutes dosing images, we can see both the substrate and the first structures of the overlayer growing on the top of the underlying layer rather than on Cu. In the monolayer regime, the self-assembly is guided by molecule-substrate interactions, while intermolecular interactions become predominant for higher coverage, even before monolayer reached saturation.

The knowledge of ASP adsorption mechanisms and of ASP coverage-dependent behavior will allow us to disentangle the contribution of ASP moiety in RGD and will help in the comprehension and interpretation of RGD characterization.

ASSOCIATED CONTENT

Supporting Information

Infrared spectra of solutions of Aspartic Acid in water at different pH

C 1s core level spectra as a function of dosing times

Thickness evaluation detailed calculations

AUTHOR INFORMATION

Corresponding Author

*E-mail: vincent.humblot@upmc.fr

Notes

The authors declare no competing financial interest.

ACKNOWLEDGMENTS

This work was supported by French state fund managed by the ANR within the Investissements d'Avenir programme under reference ANR-11-IDEX-0004-02, and more specifically within the framework of the Cluster of Excellence MATISSE

REFERENCES

(1) Méthivier C.; Humblot V.; Pradier C.-M. UHV Deposition of the Gly-Pro Dipeptide on Cu(110) by Sublimation or Electrospray Ionization. *J. Phys. Chem. C* **2016**, *120*, 27364-27368.

(2) Méthivier C.; Cruguel H.; Costa D.; Pradier C.-M.; Humblot V. Tuning the Surface Chirality of Adsorbed Gly-Pro Dipeptide/Cu(110) by Changing Its Chemical Form via Electrospray Deposition. *Langmuir* **2016**, *32*, 13759-13763.

(3) Zhang Z.; Lai Y.-X.; Yu L.; Ding J.-D. Effects of Immobilizing Sites of RGD Peptides in Amphiphilic Block Copolymers on Efficacy of Cell Adhesion. *Biomaterials* **2010**, *31*, 7873-7882.

(4) Hasselström J.; Karis, O.; Weinelt M.; Wassdahl N.; Nilsson A.; Nyberg M.; Pettersson L. G. M.; Samant M. G.; Stöhr J. The Adsorption Structure of Glycine Adsorbed on Cu(110); Comparison with Formate and Acetate Cu(110). *Surf. Sci.* **1998**, *407*, 221-236.

(5) Zhao X.; Yan H.; Zhao R. G.; Yang W. S. Self-Assembled Structures of Glycine on Cu(111). *Langmuir*, **2003**, *19*, 809-813.

(6) Löfgren P.; Krozer A.; Lausmaa J.; Kasemo B. Glycine on Pt (111): a TDS and XPS Study. *Surf. Sci.* **1997**, *370*, 277-292.

(7) Gao F.; Li Z.; Wang Y.; Burkholder L.; Tysoe W. T. Chemistry of Glycine on Pd(111): Temperature-Programmed Desorption and X-ray Photoelectron Spectroscopic Study. *J. Phys. Chem. C*, **2007**, *111*, 9981–9991.

(8) Zhao X.; Yan H.; Zhao R. G.; Yang W. S. Physisorption-Induced Surface Reconstruction and Morphology Changes: Adsorption of Glycine on the Au(110) 1 × 2 Surface. *Langmuir* **2002**, *18*, 3910-3915.

(9) Rankin R. B.; Sholl D. S. Structures of Dense Glycine and Alanine Adlayers on Chiral Cu(3,1,17) Surfaces. *Langmuir* **2006**, *22*, 8096-8103.

(10) Azevedo R. A.; Lancien M.; Lea P. J. The Aspartic Acid Metabolic Pathway, an Exciting and Essential Pathway in Plants. *Amino Acids* **2006**, *30*, 143-162.

(11) Han S.; Liu Y.; Nie X.; Xu Q.; Jiao F.; Li W.; Zhao Y.; Wu Y.; Chen C. Efficient Delivery of Antitumor Drug to the Nuclei of Tumor Cells by Amphiphilic Biodegradable Poly(L-Aspartic Acid-co-Lactic Acid)/DPPE Co-Polymer Nanoparticles. *Small* **2012**, *8*, 1596-1606.

(12) Piana S.; Jones F.; Gale J. D. Aspartic Acid as a Crystal Growth Catalyst. *CrystEngComm* **2007**, *9*, 1187-1191.

(13) Yu J.-C.; Zhao F.-G.; Shao W.; Ge C.-W.; Li W.-S. Shape-Controllable and Versatile Synthesis of Copper Nanocrystals with Amino Acids as Capping Agents. *Nanoscale*, **2015**, *7*, 8811-8818.

(14) Tan Y. N.; Lee J. Y.; Wang D. I. C. Aspartic Acid Synthesis of Crystalline Gold Nanoplates, Nanoribbons and Nanowires in Aqueous Solutions. *J. Phys. Chem. C*, **2008**, *112*, 5463–5470.

(15) Rafey A.; Shrivastavaa K. B. L.; Iqbal S. A.; Khan Z. Growth of Ag-Nanoparticles Using Aspartic Acid in Aqueous Solutions. *J. Coll. Int. Sci.* **2011**, *354*, 190-195.

(16) Guo Y. -N.; Lu X.; Zhang H.-P.; Weng J.; Watari F.; Leng Y. DFT Study of the Adsorption of Aspartic Acid on Pure, N-Doped, and Ca-Doped Rutile (110) Surfaces. *J. Phys. Chem. C* **2011**, *115*, 18572-18581.

(17) Parikh S. J.; Kubicki J. D.; Jonsson C. M.; Jonsson C. L.; Hazen R. M.; Sverjensky D. A.; Sparks D. L. Evaluating Glutamate and Aspartate Binding Mechanisms to Rutile (alpha-TiO_2) via ATR-FTIR Spectroscopy and Quantum Chemical Calculations. *Langmuir* **2011**, *27*, 1778-1787.

(18) Greiner E.; Kumar K.; Sumit M.; Giuffre A.; Zhao W.; Pedersen J.; Sahai N.; Adsorption of L-Glutamic Acid and L-Aspartic Acid to Gamma-Al_2O_3. *Geochim. Cosmochim. Acta* **2014**, *133*, 142-155.

(19) Wilson K. E.; Baddeley C. J. Understanding the Surface Chemistry of Enantioselective Heterogeneous Reactions: Influence of Modification Variables on the Interaction of Methylacetoacetate with (S)-Aspartic Acid Modified Ni{111}. *J. Phys. Chem. C* **2009**, *113*, 10706-10711.

(20) Wilson K. E.; Trant A. G.; Baddely C. J.; Interaction of the Pro-Chiral Molecule, Methylacetoacetate, with (S)-Aspartic Acid Modified Ni{111}. *J. Phys. Chem. C* **2012**, *116*, 1092-1098.

(21) Yun Y.; Gellman A.; Enantioselective Separation on Naturally Chiral Metal Surfaces: D, L-Aspartic Acid on Cu(3,1,17)(R&S) Surfaces. *Angew. Chem. Int. Ed.* **2013**, *52*, 3394 –3397.

(22) Yun Y.; Gellman A. Adsorption-Induced Auto-Amplification of Enantiomeric Excess on an Achiral Surface. *Nat. Chem.* **2015**, *7*, 520-525.

(23) Reinicker A. D.; Therrien A. J.; Lawton T. J.; Ali R.; Sykes E. C. H.; Gellman A. J. Influence of Step Faceting on the Enantiospecific Decomposition of Aspartic Acid on Chiral Cu Surfaces Vicinal to Cu{111}. *Chem. Comm.* **2016**, *52*, 11263-11266.

(24) Yun Y.; Gellman A.; Enantiospecific Adsorption of Amino Acids on Naturally Chiral Cu{3,1,17}(R&S) Surfaces. *Langmuir* **2015**, *31*, 6055-6063.

(25) Mhatre B. S.; Dutta S.; Reinicker A.; Karagoza B.; Gellman A. J. Explosive Enantiospecific Decomposition of Aspartic Acid on Cu Surfaces. *Chem. Comm.* **2016**, *52*, 14125-14128.

(26) Tanuma, S.; Powell, C. J.; Penn, D. R. Calculations of Electron Inelastic Mean Free Paths (IMFPs). 6. Analysis of the Gries Inelastic Scattering Model and Predictive IMFP Equation. *Surf. Interface Anal.* **1997**, *25*, 25-35.

(27) Roddick-Lanzilotta A. D.; McQuillan A. J. An In-Situ Infrared Spectroscopic Study of Glutamic Acid and of Aspartic Acid Adsorbed on TiO_2: Implications for the Biocompatibility of Titanium. *J. Coll. Int. Sci.* **2000**, 227, 48-54.

(28) Tabatabaei J.; Sakkakini B. H.; Watson M. J.; Waugh K. C. The Detailed Kinetics of the Desorption of Hydrogen from Polycrystalline Copper Catalysts. *Catal. Lett.* **1999**, *59*, 143-149.

(29) Clark D. T.; Peeling J.; Colling L. Experimental and Theoretical Investigation of Core Level Spectra of a Series of Amino-Acids, Dipeptides and Polypeptides. *Biochim. Biophys. Acta* **1976** *453*, 533-545.

(30) Feyer V.; Plekan O.; Tsud N.; Chab V.; Matolin V.; Prince K. C. Adsorption of Histidine and Histidine-Containing Peptides on Au(111). *Langmuir* **2010**, *26*, 8606-8613.

(31) Méthivier C.; Humblot V.; Pradier C.-M. L-Methionine Adsorption on Cu(110), Binding and Geometry of the Amino Acid as a Function of Coverage. *Surf. Sci.* **2015**, *632*, 88-92.

(32) Méthivier C.; Lebec V.; Landoulsi J.; Pradier C.-M. Probing the Binding Mechanism of Peptides on a Copper Surface: Multi layer Self-Assembly Promoted by Glutamate Residues. *J. Phys. Chem. C* **2011**, *115*, 4041-4046.

(33) Vallée A.; Humblot V.; Méthivier C.; Pradier C. - M.; Adsorption of Di- and Tripeptides on Au(110) under Ultrahigh Vacuum Conditions. 1. Polarization Modulation Reflection

Absorption Infrared Spectroscopy and X-Ray Photoelectron Spectroscopy Characterization. *J. Phys. Chem. C* **2009**, *113*, 9336-9344.

(34) Gonella G.; Terreni S.; Cvetko D.; Cossaro A.; Mattera L.; Cavalleri O.; Rolandi R.; Morgante A.; Floreano L.; Canepa M.; UHV Deposition of L- Cysteine on Au(110) Studied by HR XPS: From Early Stages of Adsorption to Molecular Organization. *J. Phys. Chem. B* **2005**, *109*, 18003-18009.

(35) Greenler R. G. Infrared Study of Adsorbed Molecule on Metal Surfaces by Reflection Techniques. *J. Chem. Phys.* **1966**, *44*, 310-315.

(36) Lorenzo M. O.; Haq S.; Bertrams T.; Murray P.; Raval R.; Baddeley C. J. Creating Chiral Surfaces for Enantioselective Heterogeneous Catalysis: *R,R*-Tartaric Acid on Cu(110). *J. Phys. Chem. B* **1999**, *103*, 10661-10669.

(37) Humblot V.; Lorenzo M. O.; Baddeley C. J.; Haq S.; Raval R. Local and Global Chirality at Surfaces: Succinic Acid versus Tartaric Acid on Cu(110). *J Am. Chem. Soc.* **2004**, *126*, 6460-6469.

(38) Feyer V.; Plekan O.; Ptasiska S.; Iakhnenko M.; Tsud N.; Prince K. C.; Adsorption of Histidine and a Histidine Tripeptide on Au(111) and Au(110) from Acidic Solution. *J. Phys. Chem. C* **2012**, *116*, 22960-22966.

(39) Barlow S. M.; Louafi S.; LeRoux D.; Williams J.; Muryn C.; Haq S.; Raval R. Supramolecular Assembly of Strongly Chemisorbed Size-and Shape-Defined Chiral Clusters: S- and R-Alanine on Cu(110). *Langmuir* **2004**, *20*, 7171-7176.

(40) Humblot V.; Méthivier C.; Raval R.; Pradier C.- M. Amino Acid and Peptides on Cu(110) Surfaces: Chemical and Structural Analyses of L-Lysine. *Surf. Sci.* **2007**, *601*, 4189-4194.

(41) Humblot V.; Tielens F.; Luque N. B.; Hampartsoumian H.; Méthivier C.; Pradier C.-M. Characterization of Two-Dimensional Chiral Self-Assemblies L- and D□Methionine on Au(111). *Langmuir* **2014**, *30*, 203-212.

(42) Jeffrey, George A. *An Introduction to Hydrogen Bonding*, Oxford University Press: Oxford, U.K., **1997**.

(43) Cruguel H.; Méthivier C.; Pradier, C.–M.; Humblot V. Surface Chirality of Gly-Pro Dipeptide Adsorbed on a Cu(110) Surface. *Chirality*, **2015**, *27*, 411-416.

TOC Graphic